Hybrid algorithm for twin image removal in optical scanning holography

P. Bhuvaneswari*

School of Electronics Engineering,
VIT University,
Chennai Campus, Vandalur,
Chennai – 600127, India
and
Department of ECE,
RajaRajeswari College of Engineering,
Bangalore – 560074, India
Email: bhuvanasamuel@gmail.com
*Corresponding author

A. Brintha Therese

School of Electronics Engineering,
VIT University Chennai Campus,
Vandalur, Chennai – 600127, India
Email: abrinthatherese@vit.ac.in

Abstract: Optical scanning holography is an incoherent optical image processing system. It is a technique, where the complete information of an object or image will be recorded as a hologram and later reconstructed to get back the original image. In the hologram reconstruction process, a virtual image is formed along with the real image, which appears as a twin image noise. To eliminate such noises, a technique of hybrid algorithm is used while recording the hologram itself. The MATLAB R2012b image processing tool is used for simulation and the simulated values are tabulated and compared with the existing method in terms of peak signal to noise ratio, mean square error. In the reconstruction, the proposed method results are having 26% increment in the MSE and PSNR values. To further improve the MSE and PSNR values a case study using different denoising techniques combined with the proposed hybrid algorithm is used and found considerable improvement of 32%. Hence the image quality is increased.

Keywords: optical scanning holography; Fresnel zone plate; optical transfer function; OTF; spatial frequency; twin image noise; denoising.

Reference to this paper should be made as follows: Bhuvaneswari, P. and Therese, A.B. (2020) 'Hybrid algorithm for twin image removal in optical scanning holography', *Int. J. Computer Aided Engineering and Technology*, Vol. 12, No. 1, pp.33–54.

Biographical notes: P. Bhuvaneswari is a Research Scholar in the School of Electronics Engineering, VIT University, Chennai, Tamilnadu, India. She is working as an Associate Professor in the Department of Electronics and Communication Engineering, Rajarajeswari College of Engineering Bangalore. She is pursuing her research in optical image processing. Her other interested research areas are digital image processing, microwave communication and antennas.

A. Brintha Therese is a Professor in the School of Electronics Engineering, VIT University, Chennai, Tamilnadu, India. She has an experience of 20 years, teaching in reputed engineering colleges in the capacity of the Head of the Department. She is an expert in optical image processing and working with MATLAB for the past 16 years. She organised many symposia and presented a number of guest lecturers all over Tamilnadu, India. She guided a number of BTech and MTech projects. She was supervising six PhD students. She is a life member of the Indian Society for Technical Education and a member of Optical Society of America. She published many papers in optical image processing and optical networking.

1 Introduction

Holography was invented in 1948 as an imaging technique (Gabor, 1948) for recording the 3D object information. In greek language 'holos' means whole and 'graphein' means to write or record hence holography means recording the whole information of an object (Poon, 1996). In digital holography the recorded hologram can be digitally stored in the computer as an interference pattern with help of charge coupled devices (CCD) (Zhenbo et al., 2015). Optical scanning holography (OSH) is an imaging technique as well as digital holography which was first suggested by Poon and Korpel (1979), in which, by means of heterodyne optical scanning, the holographic information of an object can be recorded and reconstructed digitally to obtain the original image (Poon, 2001). The importance of OSH is bypassing the use of film recording. It is an incoherent optical image processing method which provides better signal to noise ratio than coherent part. OSH has the ability to generate hologram for the fluorescent emission distributed in a 3D structure (Indebetouw et al., 2006). Tsang et al. (2015) stated to acquire wide field scenes and high resolution holograms OSH technique can be used and also demonstrated compressed OSH in which the time taken to acquire the hologram is less.

Nowadays there are many advantages in OSH than 3D sectioning methods since it will generate a 3D hologram from 2D scanning (Kuo and Tsai, 2003). OSH principle is used in applications like 3D holographic microscopy, optical recognition of 3D objects, 3D optical remote sensing, 3D holographic TV and display, 3D optical scanning cryptography (Poon, 2004), medical image recognition (Therese and Sundaravadivelu, 2012). In this paper removal of twin image in OSH leads to enhancement. Hence OSH can be considered as a pre processing method in image processing. This paper is organised as follows, in Section 2 related work is discussed, in Section 3 proposed method and algorithm are explained, simulation results and the performance analysis are discussed in Sections 4 and 5, followed by case study in Section 6.

2 Related work

In OSH while reconstructing the hologram there is a presence of twin image which is considered as a noise. According to McElhinneya et al. (2008). The twin-image can be segmented and filtered after reconstruction. A method is explained by Lee et al. (2015) in which hologram acquisition is based on time resolved heterodyne analysis. Park et al. (2005) demonstrated the optical reconstruction using amplitude only Spatial Light Modulators and phase only spatial light modulators. Twin image and background noises are eliminated. Since OSH is an incoherent imaging technique, it is able to overcome the spatial resolution limit by adding the offaxis scanning hologram with a pupil larger than the object demonstrated by Rosen et al. (2012). Kim (1997) proved in his article OSH for 3D imaging that acquisition of hologram without speckle noise and twin image noise is possible. Twin image elimination is achieved through recovering the phases of diffraction in less intensity signals (Chen et al., 2016). To remove the twin image an iterative algorithm is suggested and its ability through simulated and real data is demonstrated. Reconstructed images of small objects from a digital hologram can be enhanced by this method (Denis et al., 2008). By using complex hologram twin-image was rejected (Poon et al., 2000). To remove the twin image, digital filtering and electronic multiplexing are used (Ke et al., 2011; Doh et al., 1996; Kim et al., 1998). n this paper a new algorithm for twin image rejection by varying the spatial frequency is proposed.

3 Proposed methodology

OSH is based on the principle of acousto optic heterodyne scanning and consists of recording and reconstruction stages. In the reconstruction of the OSH which was demonstrated by Poon experienced some noise in the form of twin image. In proposed method to remove the twin image noise and also to improve the image quality a hybrid algorithm is used. In this proposed algorithm while recording the hologram the combination of new OTF and conventional OTF by varying the spatial frequency (kx, ky) along with depth parameter ($z = 2\sigma k_0$) keeping wavelength of the light λ(633 nm) is constant. Then the resultant updated hologram is reconstructed with the help of simulation and the results are obtained and compared.

3.1 Optical scanning holography (experimental setup)

The experimental setup of OSH (Figure 1). Collimated laser is used to light up the pupil $P_1(x, y)$ at the frequency of 'f'. Another pupil $P_2(x, y)$ is illuminated by the laser with '$f + \omega$'. Acousto optic frequency shifter (AOFS) is used to create a different temporal frequency ω. In the recording stage 3D object or 2D image is being scanned by a two dimensional time dependant Fresnel zone plate (TDFZP) which is formed by the waves from beam splitters BS1 and BS2 at different temporal frequencies(f, ω). The two dimensional sine and cosine FZP hologram is generated using TDFZP. In this paper when the test image is scanned by 2D mirror the amount of light transmitted through the image is collected by the photo multiplier and the resultant heterodyned current I_ω (x, y) is delivered as the output. This current contains the hologram information of the input

image. It is mixed with cosωt or sinωt to obtain the in phase and quadrature components of the demodulated current respectively as the reconstruction part

The OTF existing along with variations in the parametric values of k_X k_Y and σ have resulted in reduction of the twin image noise. When adding the OTF new as a feed forward component, the gain margin of the response is reduced and the noise present in the OTF existing is thereby reduced. This feed forward addition is a result of generating a noiseless reconstruction of the hologram.

Figure 1 OSH experimental setup

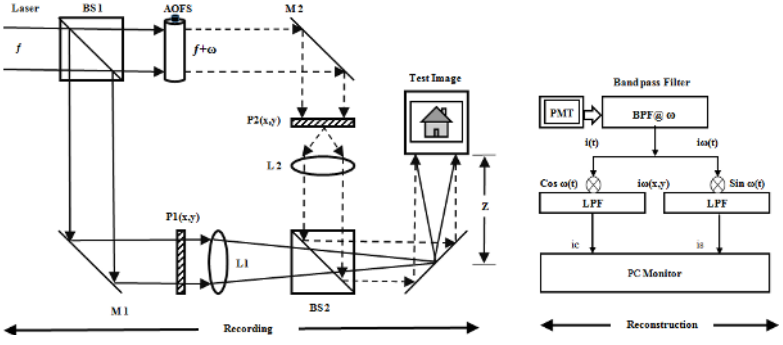

Notes: BS1, BS2 – beam splitters; M1, M2 – mirrors; AOFS – acousto optic frequency shifter; L1, L2 – lense; PMT – photo multiplayer; P1(x, y) = P2(x, y) – pupils.

Source: Poon (2001)

3.2 Algorithm

The proposed method also consists of recording and reconstruction stages. In order to generate the updated hologram (recording) and to reconstruct the test image with a better quality compared to the existing method hybrid algorithm is used. The steps which are used in creating the new OTF is shown as the flow chart (Figure 2):

Step 1 Reading the parameters k_x, k_y, σ, λ, M, R, C

Step 2 Calculate OTF Existing

Step 3 Vary k_x, k_y and *sigma*

Step 4 Calculate New OTF

Step 5 Add existing and new OTF to obtain the updated hologram

Step 6 Obtain the complex conjugate of updated hologram

Figure 2 Flowchart for finding new OTF

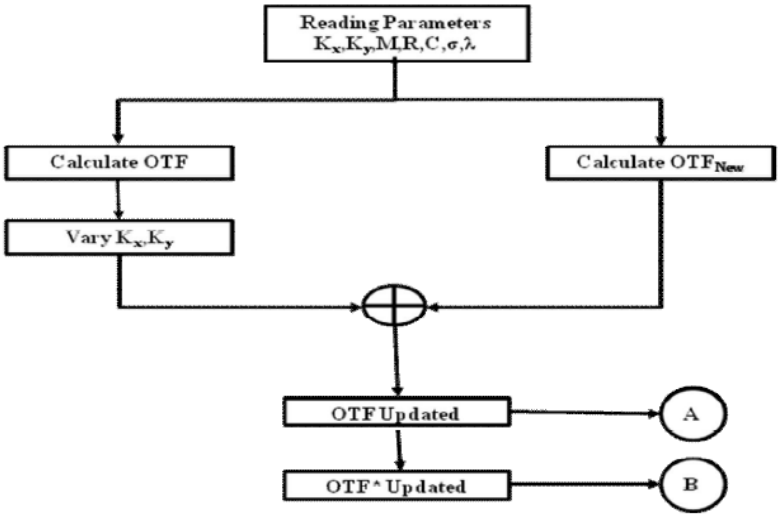

Figure 3 Flow chart-two stages of OSH

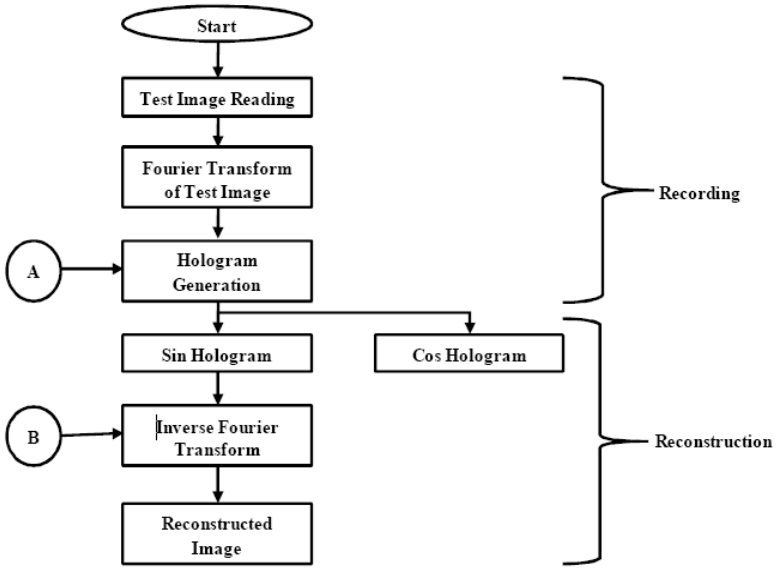

Figure 3 explains about the updated hologram generation (recording) and reconstruction stages of OSH. Here Sin hologram is taken into considerations and the resultant reconstructed image did not have the twin image noise effect.

As shown in (Figure 1) two pupils like $P_1(x, y) = P_2(x, y) = \delta(x, y)$, are chosen. The OTF of the optical scanning system is given by,

$$OTP\omega\left(k_x, k_y : z\right) : \exp\left[-j\frac{z}{2k_0}\left(\begin{matrix}2\\k_x\end{matrix} + \begin{matrix}2\\k_y\end{matrix}\right)\right] \tag{1}$$

$$= OTF_{OSH}\left(k_x, k_y : z\right) \tag{2}$$

where

z depth parameter measured away from the scanning mirror

ko $\frac{2\prod}{\lambda}$; wave number of the light

k_x, k_y spatial frequencies

λ 633 nm.

The subscript OSH means the OTF of the holographic recording.

The test image $t(x, y)$ was recorded as a two dimensional hologram and the recorded hologram can be written as:

$$t(x, y) = Re\left[\int_F^{-1}\left\{F\left\{\left|\Gamma_0\left(k_x, k_y : z\right)\right|^2\right\} OTF_{OSH}\left(k_x, k_y : z\right)\right\} dz\right] \tag{3}$$

The holographic recording is written in terms of impulse response:

$$t(x, y) = Ro\left[\left|\Gamma_0\right|^2 * h(x, y : z) dz\right] \tag{4}$$

where $|\Gamma_0|$ represents light intensity distribution:

$$\left|\Gamma_0\right|^2 = \delta\left(x - x_0\right)^2 + \left(y - y_0\right)^2 \tag{5}$$

The sine-Fresnel zone plate (sine-FZP) hologram and cosine-Fresnel zone plate (cosine-FZP) hologram is given by equations (6) and (7).

$$^{t}\sin(x, y) = \mathrm{Re}\left[\int h\left(x, y : z\right) \otimes \left|\Gamma_0\right|^2 dz\right] \tag{6}$$

$$^{t}\cos(x, y) = \mathrm{Im}\left[\int h\left(x, y : z\right) \otimes \left|\Gamma_0\left(x, y : z\right)\right|^2 dz\right] \tag{7}$$

In the proposed method sine-FZP hologram of the test image is used for further reconstruction. The twin image exists upon the reconstruction hence to remove the twin image in the simulation we have modified the spacial frequencies k_x, k_y in the optical transfer function and created the OTF_{new} is given by:

$$OTF_{new} = \exp\left[-j * 2\pi * \frac{Z}{2k_0}\left(\sqrt{\begin{matrix}2\\k_x\end{matrix} + \begin{matrix}2\\k_y\end{matrix}}\right)\right] \tag{8}$$

$$k_x = -\left(\frac{1}{\lambda}\right)^2 - \left[\left(R - \left(\frac{M}{2}\right) - 1\right)\delta f\right] \tag{9}$$

$$k_y = \left[\left(C - \left(\frac{M}{2}\right)\right)\delta f\right] \tag{10}$$

where

R, C image matrix

M image size

δf scale factor.

The need for inducing new expressions for k_x, k_y is the inherent problem with spatial frequencies. The lower the spatial frequency the lesser data carried by it. Since the image size is being reduced from 1,024 pixels to 512 pixels, the compression itself allows for loss of data from the pixels. This causes the image sharpness to be blurred around the edges and allows for a spatial frequency that can be represented using a sine wave. The drawback of the sine wave frequency causes the image components to be out of focus. In order to overcome this deficit a new equation for regenerating the k_x, k_y values are introduced in equations (9) and (10). It converts the sine wave into a square wave estimate. This conversion intermittently improves the image sharpness at lower resolutions.

The hybrid hologram is obtained by adding the OTF_{osh} (1) and OTF_{new} (8) and the updated hologram of the test image $t(x, y)$ is given by:

$$t(x, y) = \mathrm{R_e}\left[\int {}_F{}^{-1}\left\{F\left\{\left|\Gamma_0\left(k_x, k_y : Z\right)\right|^2\right\} OTF_{new}\left(k_x, k_y : Z\right)\right\} dz\right] \tag{11}$$

In frequency domain holographic recording process can be interpreted as the spectrum of the image along with depth (z) which is processed by OTF_{new}. In the reconstruction process the quality of the image is increased by the addition of both OTFs.

4 Simulation results

Input brain image and impulse response of OSH are shown [Figures 4(a) and 4(b)]. Figures 4(c) and 4(d) represents the sine and cosine FZP holograms respectively, obtained in existing method. Reconstructed hologram images from the existing method and proposed method are shown respectively [Figures 4(e) and 4(f)]. The constants of equation (8) are combined together and named as 'σ'= $\pi z/k_o$ for simulation purpose. The existing method hologram which is created using OTF_{osh} is added with the hologram which is obtained from OTF_{new}, resulting an upgraded hologram. After many experiments for a wide range of k_x, k_y and σ, we have arrived to an optimal value of σ = 0.001, $k_x = k_y = -5$ gave better MSE and PSNR.

Figure 4 (a) Input image (b) Impulse response of OSH (c) Sin FZP hologram (d) Cosine FZP hologram (e) Existing method reconstruction of sine hologram k_x, k_y = –12.8 and σ = 0.51twin image noise exists (f) Reconstruction of sine hologram in proposed method k_x, k_y –5 and σ = 0.001 no. twin image noise

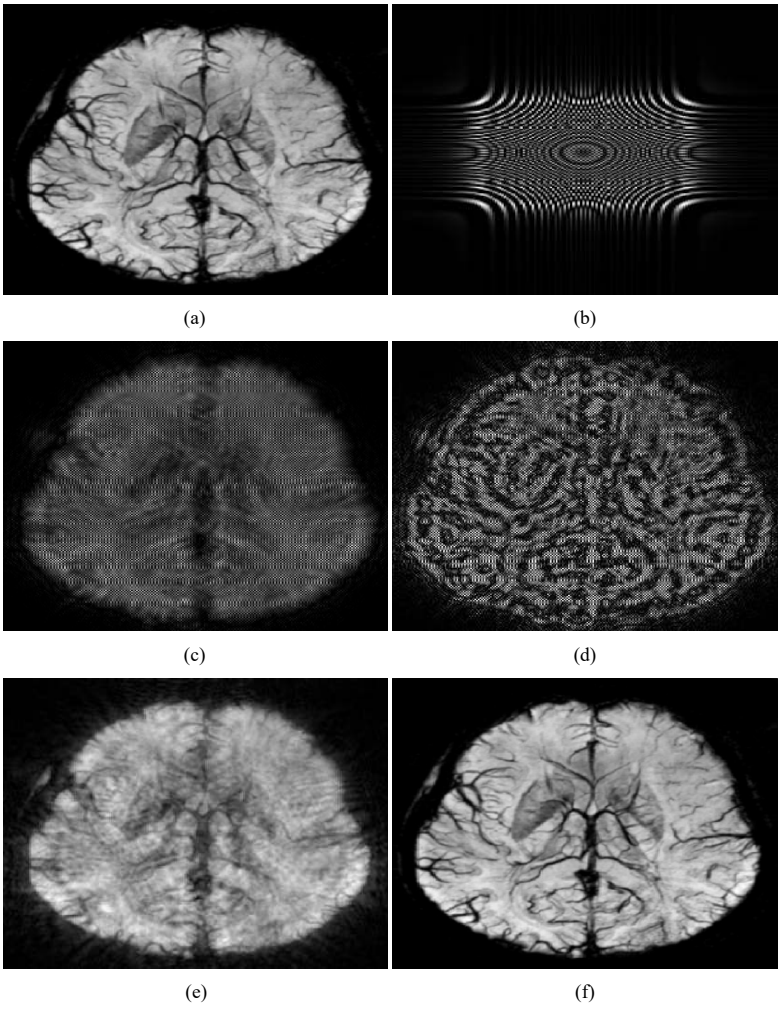

(a) (b)

(c) (d)

(e) (f)

5 Performance analysis

We have evaluated the obtained reconstructed images rather than visual inspection in a quantitative manner by measuring PSNR and MSE.

If image pixels are represented with 8 bit and signals are represented as 255, the PSNR may be defined as the ratio of maximum signal power to the corrupted signal:

$$PSNR = 10 * \log_{10}\left(\frac{255^2}{MSE}\right) \tag{12}$$

where

$$MSE = \frac{1}{MN}\sum_{i=0}^{M-1}\sum_{j=0}^{N-1}\left[x(i,\, j) - y(i,\, j)\right]^2 \tag{13}$$

Here $x(i, j)$ is the original image and $y(i, j)$ is the retrieved image and M, N are the size of the image.

The results are tabulated and compared with existing method for various images. The results are shown in Tables 1 and 2. To generate the hologram, the standard OTF is studied and analysed along with basic parameters like σ, k_x, k_y which are shown in Table 1.

The experiment is done for wide range of kx, ky from –500 to +500, and σ from 10 to 0.001 some of them are tabulated in Table 1 for reference. We concluded that the optimal value of k_x, k_y = –5 and σ = 0.001 gave better results.

Table 1 Evaluation of MSE and PSNR for wide range of k_x, k_y and σ for reference brain image

k_x, k_y	σ	*MSE*	*PSNR (dB)*
–500	10	0.4214	51.8834
	1	0.4214	51.8834
	0.001	0.4214	51.8834
–100	10	0.4214	51.8834
	1	0.4214	51.8834
	0.001	0.4214	51.8834
–50	10	0.4432	51.6644
	1	0.4241	51.8858
	0.001	0.0345	62.7478
–5	10	0.4436	51.6607
	1	0.4236	51.8608
	0.001	*0.0193*	*65.2721*
5	10	0.5786	50.5073
	1	0.5939	50.3940
	0.001	0.4215	51.8832
50	10	0.4214	51.8834
	1	0.4214	51.8834
	0.001	0.4215	51.8829

Table 1 Evaluation of MSE and PSNR for wide range of k_x, k_y and σ for reference brain image (continued)

k_x, k_y	σ	*MSE*	*PSNR (dB)*
100	10	0.4214	51.8834
	1	0.4214	51.8834
	0.001	0.4215	51.8834
500	10	0.4214	51.8834
	1	0.4214	51.8834
	0.001	0.4234	51.8834

Table 2 Comparison between existing and proposed method for various images (see online version for colours)

Type of image	*Proposed method*		*Existing method*		*% increment*	
	MSE	*PSNR (dB)*	*MSE*	*PSNR (dB)*	*MSE*	*PSNR*
Brain image	0.0193	65.2721	0.4214	51.8834	95.8	25.8
Chest X-ray	0.2181	54.7446	0.7031	49.6608	68.9	10.2
Spinal CT1	0.0043	71.7701	0.0432	61.7774	90.0	16.1
Spinal CT2	0.2783	53.6766	0.5669	50.5958	50.9	6.0
Angiogram	0.0003	82.9210	0.8497	48.8382	99.9	69.7
Average increment					81.12%	25.56%

Figure 5 Comparison of PSNR for various images (see online version for colours)

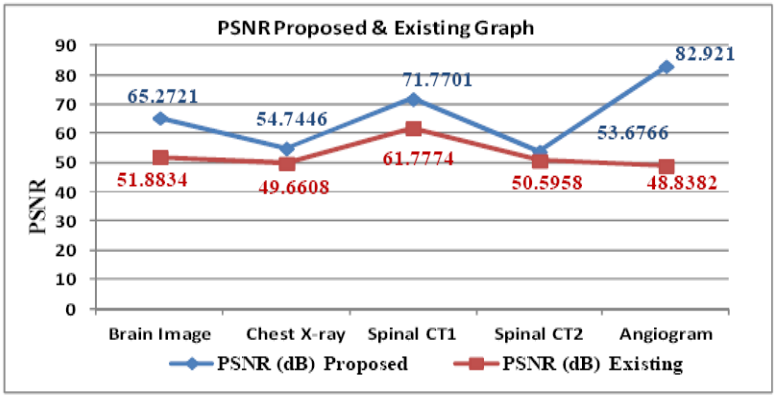

For the given brain image the comparison of PSNR and MSE for various range of k_x, k_y with fixed $\sigma = 0.001$ is shown in Figures 5 and 6. Compared with the existing method the proposed method gives 26% increment of PSNR and better MSE. This algorithm holds good for other medical images like chest x-ray, spinal CT, angiogram etc. The proposed method is tested for various images and the results are shown in Table 2. While

comparing the MSE is very low (0.0003) than existing method, which indicates that the robustness of the image is increased. The visual quality of the reconstructed images is consistent with the quantitative evaluations.

The figures indicate the MSE, PSNR value for various images. The proposed algorithm resulting on low MSE values and considerable increase in PSNR values. But at the same time it was evident that with this technique we can achieve up to 26% improvement on MSE and PSNR against the conventional methodology.

Figure 6 Comparison of MSE for various images (see online version for colours)

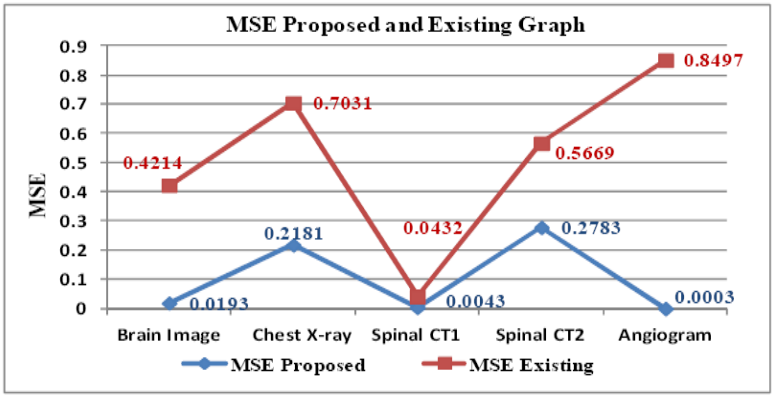

6 Case study

6.1 Denoising technique

In a quest to further improve the PSNR value, after going through a lots and lots of Literature surveys (Bhuvaneswari et al., 2014; Tahoces et al., 1991; Kundu, 2013; Prabhpreet et al., 2016; Kumar and Datta, 2016; Ali, 2016; Mozammel et al., 2016) it was found, using denoising technique would have a considerable impact on the PSNR value. In the wake of doing a statistical analysis, we are considering chest x-ray images as the source in this case study since medical x-ray images are naturally low contrast, low brightness and having noise.

The following tabulations demonstrates the impact of inducing the said noises:

1 speckle

2 salt and pepper

3 Gaussian

4 poison.

And then de-noising the same with the said filters:

1 circular average filter

2 Weiner filter

3 median filter

4 average filter

5 Gaussian filter

6 Haar filter.

After denoising the proposed method is applied. The outcome of this technique proved to have a significant impact in improving the quality of the chest x-ray image. Figure 7 and Figure 8 visually indicated the effect of hybrid algorithm. The combination of input image, noisy image, OSH reconstructed image for two different noises like Gaussian, Salt and Pepper are shown in Figures 7 and 8.

Figure 7 (a) Input image (b) Gaussian noisy image (c) OSH reconstructed image

(a) (b) (c)

Figure 8 (a) Input image (b) Salt and pepper noisy image (c) OSH reconstructed image

(a) (b) (c)

Table 3 Case study result

Speckle noise PSNR												
Noise level sigma	*CAF*		*Weiner*		*Median*		*Average*		*Gaussian*		*Haar*	
	Denoised	*Proposed*	*Denoised*	*Proposed*	*Denoised*	*Proposed*	*Denoised*	*Proposed*	*Denoised*	*Proposed*	*Denoised*	*Proposed*
0	34.76	*65.07*	41.19	*65.09*	38.65	*65.10*	35.55	*65.08*	37.81	*65.11*	34.77	*43.36*
0.01	27.93	*64.84*	36.71	*65.10*	33.01	*65.02*	33.67	*65.08*	31.58	*65.02*	27.91	*43.37*
0.01	25.07	*64.59*	33.12	*65.10*	30.27	*64.94*	32.17	*65.12*	28.79	*64.96*	25.08	*43.37*
0.02	22.31	*64.22*	29.72	*65.14*	27.48	*64.82*	30.12	*65.17*	26.03	*64.86*	22.32	*43.37*

Table 3 Case study result (continued) (see online version for colours)

Salt n pepper noise PSNR												
Noise level sigma	*CAF*		*Weiner*		*Median*		*Average*		*Gaussian*		*Haar*	
	Denoised	*Proposed*	*Denoised*	*Proposed*	*Denoised*	*Proposed*	*Denoised*	*Proposed*	*Denoised*	*Proposed*	*Denoised*	*Proposed*
0	34.39	*65.08*	33.96	*65.04*	43.95	*65.12*	35.41	*65.10*	37.93	*65.12*	36.83	*43.36*
0.01	27.10	*64.81*	28.54	*64.88*	43.89	*65.12*	33.56	*65.11*	31.30	*65.05*	32.31	*43.35*
0.01	24.45	*64.55*	26.01	*64.73*	43.83	*65.12*	32.00	*65.13*	28.20	*64.96*	29.87	*43.34*
0.02	21.28	*63.98*	24.12	*64.58*	43.71	*65.12*	29.80	*65.18*	25.37	*64.80*	27.24	*43.33*

Table 3 Case study result (continued)

Gaussian noise PSNR													
Noise level sigma	*CAF*		*Weiner*		*Median*		*Average*		*Gaussian*		*Haar*	
	Denoised	*Proposed*	*Denoised*	*Proposed*	*Denoised*	*Proposed*	*Denoised*	*Proposed*	*Denoised*	*Proposed*	*Denoised*	*Proposed*
0	20.75	*63.97*	29.54	*65.34*	28.04	*64.88*	28.33	*65.31*	24.32	*64.85*	26.04	*43.36*
0.01	20.73	*63.91*	29.42	*65.28*	27.88	*64.81*	28.22	*65.22*	24.29	*64.76*	26.00	*43.41*
0.01	20.66	*63.83*	29.07	*65.17*	27.65	*64.70*	27.98	*65.15*	24.15	*64.66*	25.85	*43.47*
0.02	20.50	*63.66*	28.13	*64.95*	26.90	*64.50*	27.24	*64.89*	23.86	*64.46*	25.30	*43.58*

Table 3 Case study result (continued)

Poison noise PSNR												
Noise level sigma	*CAF*		*Weiner*		*Median*		*Average*		*Gaussian*		*Haar*	
	Denoised	*Proposed*	*Denoised*	*Proposed*	*Denoised*	*Proposed*	*Denoised*	*Proposed*	*Denoised*	*Proposed*	*Denoised*	*Proposed*
0	27.32	*60.66*	24.51	*52.82*	24.05	*62.30*	24.39	*61.37*	28.79	*61.53*	24.47	*43.46*
0.01	27.26	*60.63*	24.51	*62.62*	24.05	*61.15*	24.40	*61.68*	28.81	*60.53*	24.47	*43.46*
0.01	27.29	*60.61*	24.51	*62.64*	24.06	*61.17*	24.40	*61.66*	28.78	*60.52*	24.47	*43.46*
0.02	27.30	*60.61*	24.51	*62.64*	24.05	*61.15*	24.40	*61.65*	28.80	*60.53*	24.46	*43.46*

Table 3 Case study result (continued)

Speckle noise MSE										
Noise level sigma	*CAF*		*Weiner*		*Median*		*Average*		*Gaussian*	
	Denoised	*Proposed*	*Denoised*	*Proposed*	*Denoised*	*Proposed*	*Denoised*	*Proposed*	*Denoised*	*Proposed*
0.001	21.74	*0.02*	4.95	*0.02*	8.87	*0.02*	18.11	*0.02*	10.77	*0.02*
0.005	104.69	*0.02*	13.88	*0.02*	32.48	*0.02*	27.95	*0.02*	45.24	*0.02*
0.01	202.13	*0.02*	31.74	*0.02*	61.05	*0.02*	39.48	*0.02*	86.00	*0.02*
0.02	381.81	*0.02*	69.41	*0.02*	116.16	*0.02*	63.27	*0.02*	162.14	*0.02*

Table 3 Case study result (continued)

Salt n pepper noise MSE												
Noise level sigma	*CAF*		*Weiner*		*Median*		*Average*		*Gaussian*			
	Denoised	*Proposed*	*Denoised*	*Proposed*	*Denoised*	*Proposed*	*Denoised*	*Proposed*	*Denoised*	*Proposed*		
0.001	23.64	*0.02*	26.15	*0.02*	2.62	*0.02*	18.69	*0.02*	10.48	*0.02*		
0.005	126.72	*0.02*	91.03	*0.02*	2.66	*0.02*	28.68	*0.02*	48.22	*0.02*		
0.01	233.17	*0.02*	162.84	*0.02*	2.69	*0.02*	41.05	*0.02*	98.39	*0.02*		
0.02	484.13	*0.03*	251.96	*0.02*	2.77	*0.02*	68.02	*0.02*	188.74	*0.02*		

Table 3 Case study result (continued)

Gaussian noise MSE										
Noise level sigma	*CAF*		*Weiner*		*Median*		*Average*		*Gaussian*	
	Denoised	*Proposed*	*Denoised*	*Proposed*	*Denoised*	*Proposed*	*Denoised*	*Proposed*	*Denoised*	*Proposed*
0.001	547.224	*0.026*	72.230	*0.019*	102.224	*0.021*	95.514	*0.019*	240.524	*0.021*
0.005	549.653	*0.026*	74.273	*0.019*	105.948	*0.021*	97.954	*0.020*	242.319	*0.022*
0.01	559.133	*0.027*	80.461	*0.020*	111.804	*0.022*	103.635	*0.020*	250.347	*0.022*
0.02	579.087	*0.028*	99.919	*0.021*	132.643	*0.023*	122.747	*0.021*	267.245	*0.023*

Table 3 Case study result (continued)

Poison noise MSE										
Noise level sigma	*CAF*		*Weiner*		*Median*		*Average*		*Gaussian*	
	Denoised	*Proposed*	*Denoised*	*Proposed*	*Denoised*	*Proposed*	*Denoised*	*Proposed*	*Denoised*	*Proposed*
0.001	120.498	*0.056*	230.394	*0.340*	256.083	*0.038*	236.429	*0.047*	85.831	*0.046*
0.005	122.075	*0.056*	230.352	*0.036*	255.818	*0.050*	236.346	*0.044*	85.617	*0.058*
0.01	121.268	*0.057*	229.960	*0.035*	255.544	*0.050*	235.977	*0.044*	86.157	*0.058*
0.02	121.031	*0.057*	230.160	*0.035*	255.684	*0.050*	236.148	*0.044*	85.772	*0.058*

Based on the results of inducing noises to the input images and then denoising using different filters after applying the proposed technique we discovered three advantages:

1 improved PSNR

2 improved MSE

3 improved execution time.

Especially this proposed method is more suitable for noisy medical images like chest x-rays. We infer from Table 2 the PSNR of chest x-ray image is boosted to 54.7446dB from 49.6608dB. In Table 3 we can observe still more improvement in PSNR with denoising up to maximum 65.12dB. This is 32% increment for PSNR. For the above-denoised filters for the various noises, the PSNR and MSE values are tabulated.

7 Conclusions

OSH is an incoherent optical image processing method in which film recording is eliminated for recording which has got plenty of applications especially in medical field. In our work we have shown that the twin image created during the reconstruction process of the hologram can be eliminated by means of this proposed hybrid algorithm and the image quality can be improved. This work can be done for cosine hologram also. This method will be applicable for the images having more noise like medical images. The various parameters like PSNR, MSE are calculated and tabulated. A case study by inducing noise and then denoising the same by using different filter was done to achieve 32 % increase in PSNR value. Hence, OSH can be considered as a pre processing method in image processing.

References

Ali, H.M. (2016) 'A new method to remove salt and pepper noise in magnetic resonance images', *IEEE International Conference on Computer Engg and Systems*, pp. 155–160.

Bhuvaneswari, P. and Therese, A.B. (2014) 'Edge detection techniques in digital and optical image processing', *IJERA*, Vol. 4, No. 5, pp.33–37.

Chen, B.K., Chen, T-Y., Hung, S.G., Huang, L-Y. and Yuan, J. (2016) 'Twin image removal in digital in-line holography based on iterative inter-projections', *Journal of Optics*, Vol. 18, No. 6, p.65602.

Denis, L., Fournier, C., Fournel, T. and Ducottet, C. (2008) 'Numerical suppression of the twin-image in in-line holography of a volume of micro-objects', *Measurement Science and Technology*, Vol. 19, p.74004, IOP Publishing, Bristol, UK.

Doh, K.B. et al. (1996) 'Twin image elimination in optical scanning holography', *Optics & Laser Technology*, Vol. 28, No. 2, pp.135–141.

Gabor, D. (1948) 'A new microscopic principle', *Nature*, No. 161, No. 4098, pp.777–779.

Indebetouw, G. et al. (2006) 'Quantitative phase imaging with scanning holography an experimental assessment', *Biomedical Engineering Online*, Vol. 5, p.63, DOI: 10.1186/1475925X-5-63

Ke, J., Poon, T-C. and Lam, E.Y. (2011) 'Depth resolution enhancement in optical scanning holography with a dual-wavelength laser source', *Applied Optics*, Vol. 50, No. 34, pp.285–296.

Kim, T. (1997) *Optical Scanning Holography for 3D Imaging of Fluorescent Objects in Turbid Media*, Doctoral Dissertation, Virginia Polytechnic Institute and State University.

Kim, T., Poon, T.C. and Indebetouw, G. (1998) 'Twin image removal by digital filtering and optical scanning holography', *Proceedings of the Thirtieth South eastern Symposium on System Theory*, IEEE, pp.191–195.

Kumar, A. and Datta, A. (2016) 'Adaptive edge discriminated median filter to remove impulse noise', *IEEE International Conference on Computing, Communication and Automation*, pp.1409–1413.

Kundu, R. (2013) 'Structural enhancement of digital x-ray image of bone with a suitable denoising technique', *IEEE International Conference on Medical Informatics and Telemedicine*, pp.17–22.

Kuo, C.J. and Tsai, M.H. (2003) *Three Dimensional Holographic Imaging*, Vol. 15, John Wiley & Sons, USA.

Lee, M. et al. (2015) 'Hologram acquisition by using time resolved heterodyne method in optical scanning holography', in *CLEO: Applications and Technology*, Optical Society of America, pp.JW2A–84.

McElhinneya, C., Hennellya, B.M., Ahrenberga, L. and Naughton, T.J. (2008) 'Removing the twin image in digital holography by segmented filtering of in-focus twin image', *Proc. Of SPIE*, Vol. 7072.

Mozammel, C., Gao, J. and Islam, R. (2016) 'Fuzzylogic based filtering for image denoising', *IEEE International Conference on Fuzzy Systems*.

Park, J. et al. (2015) 'An optical reconstruction of hologram recorded by OSH using amplitude only SLM and phase only SLM', *IEEE 3DTV Conference*.

Poon, T.C. (2001) *Contemporary Optical Image Processing with MATLAB*, Elsevier Science, Netherland.

Poon, T.C. (2004) 'Recent progress in optical scanning holography', *Journal of Holography*, Vol. 1, No. 1, pp.6–25.

Poon, T.C. and Korpel, A. (1979) 'Optical transfer function of acoustic-optic heterodyning image processor', *Optics Letters*, Vol. 4, No. 10, pp.317–319.

Poon, T.C., Kim, T., Indebetouw, G., Schilling, B.W., Wu, M.H., Shinoda, K. and Suzuki, Y. (2000) 'Twin image elimination experiments for three-dimensional images in optical scanni Holography', *Optics Letters*, Vol. 25, No. 4, pp.215–217.

Poon, T-C., Wu, M.H., Shinoda, K. and Suzuki, Y. (1996) 'Optical scanning holography', *Proceedings of IEEE*, Vol. 84, No. 5, pp.753–764.

Prabhpreet, K., Singh, G. and Kaur, P. (2016) 'Image enhancement of ultra sound images using multifarious denoising filters and GA', *IEEE International Conference on Advances in Computing, Communications and Informatics*, pp 2375–2384.

Rosen, J., Natan, T.S., Katz, B. and Brooker, G. (2012)'Approaches to overcome the resolution problem in incoherent digital holography', *Optical Imaging and Metrology: Advanced Technologies*, Wiley Publishers, Germany

Tahoces, P.G., Correa, J., Souto, M., Gonzalez, C., Gomez, L. and Vidal, J.J. (1991) 'Enhancement of chest and breast radiographs by automatic spatial filtering', *IEEE Transactions of Medical Imaging*, Vol. 10, No. 3 pp.330–335.

Therese, A.B. and Sundaravadivelu, S. (2012) 'Detection of micro calcification in mammograms using optical scanning holography', *International Journal of Signal Processing, Image Processing & Pattern Recognition*, Vol. 5, No. 1, pp.99–112.

Tsang, P.W.M., Liu, J-P. and Poon, T.C. (2015) 'Compressive optical scanning holography', *Optica*, Vol. 2, No. 5, pp.476–483.

Zhenbo, R., Chen, N., Chan, A.C.S and Lam, E.Y. (2015) 'Extended focused imaging in a holographic microscopy imaging system', *IEEE International Conference in Imaging Systems and Techniques*, pp.1–6.